Evaluation of Rockfall Hazard Based On UAV Technology And 3D Rockfall Simulations

Mustafa Utlu (utlumus@gmail.com)
Bingol University: Bingol Universitesi https://orcid.org/0000-0002-7508-4478
Muhammed Zeynel ÖZTÜRK
Niğde Ömer Halisdemir University: Nigde Omer Halisdemir Universitesi
Mesut Şimşek
Hatay Mustafa Kemal University: Hatay Mustafa Kemal Universitesi

Research Article

Keywords: Rockfalls, Hazard, RAMMS, 3D modelling, UAV

Posted Date: July 9th, 2021

DOI: https://doi.org/10.21203/rs.3.rs-681240/v1

Abstract

In this study, the rockfall hazard in Hacıabdullah village located in the Central Anatolia region of Turkey was assessed with three-dimensional (3D) rockfall analyses based on unmanned aerial vehicle (UAV) technology. With several rockfall disasters experienced in the village, the final event occurred as severe rockfall in 2008 and several houses were evacuated due to rockfall risk after this event**.** In order for the rockfall hazard to be assessed close to reality in the study area, rocks with falling potential identified in the field were assessed using high-resolution digital surface model (DSM) data produced from images obtained with UAV. During field studies, 17 rocks with fall hazard were identified and dimensional measurements were performed. According to dimensional values, the geometric and volumetric features of each rock were assessed close to reality with the RAMMS 3D rockfall modelling program. As a result of modelling, the kinetic energies of the rocks were identified to reach up to 3476 kJ, with velocities of up to 23.1 m/s and bounce heights of up to 14.57 m. On steep slopes rocks do not travel very long distances; however, in gentle slopes, they were identified to be able to roll very long distances. Rocks that do not move very far from the source are; in other words, where the fall process is dominant, may create damage on roads mainly. However, those with the feature of rolling, in other words, blocks which can travel long distances from the source area, have the potential to cause great damage to settlement areas, roads and trees. According to the hazard map, modelling of rock blocks numbered R6, R12, R13, R14, R15, R16 and R17 showed settlement units were within the high and moderate risk areas.

Introduction

Rockfalls are one of the most dangerous natural disasters experienced on earth (Varnes 1978; Evans and Hungr 1993; Liu et al. 2021). Rockfalls, which are very difficult to predict in terms of occurrence time and pattern are one of the mass movements causing most damage and loss of life. Falling rocks cause great damage to areas like roads, settlement units and infrastructure, in addition to causing great risk for human life (Tanarro and Munoz 2012; Lu et al. 2019; Utlu et al. 2020a). Rockfalls have high potential to occur rapidly and suddenly at different angles and occur in nearly all conditions and different rock groups (Fityus et al. 2013; Singh et al. 2016; Gül et al. 2016). The basic source area for rockfalls are vertical or almost vertical rock faces (Varnes 1978; Evans and Hungr 1993).

Many factors affect rockfalls in these high-slope areas and these factors are divided into 3 groups. These are (1) structural features like gravity, slope-aspect-elevation features, discontinuous surfaces on the slope, and lithologic features, (2) environmental factors like climate (rainfall, freeze-thaw events, wind, snowmelt, etc.), vegetation root development, tectonism and weathering features, and (3) anthropogenic factors like road construction, wrong engineering practices, explosives used during mine excavations, and building-foundation work (Bull et al. 1994; Mccarroll et al. 1998; Matsuoka 1999; Ashfield 2001; Vidrih et al. 2001; Dorren 2003; Yılmaz et al. 2008; Abebe et al. 2010; Vijayakumar et al. 2011; Cybulski 2014; Youssef et al. 2015; Aydın and Eker 2017).

Rockfall events frequently occur in Turkey, at different locations and elevations, in settlement units founded in both mountainous areas and near high slopes. Rockfall events are the most frequent natural disasters after earthquakes, landslides and floods in Turkey and lead the topics studied in Turkey (Taga and Zorlu 2016; Dinçer et al. 2016; Gül et al. 2016; Aydın and Eker 2017; Geniş et al. 2017; Kayabaşı 2018; Akın et al. 2019, 2021; Utlu et al. 2021, 2020a, b). This study investigated the rockfall hazard in Hacıabdullah village located in Niğde province in Central Anatolia which has experienced rockfalls both in the past and at present. Rockfall hazard were assessed with three-dimensional (3D) rockfall analyses using high-resolution digital surface modelling (DSM) data based on images taken with an unmanned aerial vehicle (UAV) of rocks identified in the field with rockfall hazard.

Study Area

Located in the Central Anatolia region of Turkey, Hacıabdullah village is within a valley formed by volcanic rocks on the east slopes of the Melendiz stratovolcano and is an area where intense rockfall events occur (Fig. 1). The village, founded under a steep slope formed by volcanic rocks containing cooling fractures, experienced many rockfall events during history and these events continue to the present day (Fig. 2). According to a report by Ministry of Interior Disaster and Emergency Management Presidency (AFAD), Hacıabdullah village has experienced several rockfall events from 1957 to the present day on different dates (05/04/1957, 26/06/1963, 13/09/1974, 21/03/1983, 13/11/2007, 03/03/2008). In the report from 1957, the decision was made to evacuate 85 families at risk from rockfalls; however, the local public did not implement this decision. A report in 1963 stated that 92 households were damaged by both rockfalls and floods. In 1974, 12 houses were affected by rockfalls. In 2007, it was recommended that 50 houses with rockfall risk be moved. During a rockfall occurring in 2008, 2 houses were damaged by rockfalls (AFAD, 2011; Fig. 2).

The study area has semi-arid climate features shown by the letters “BSk” according to the Köppen-Geiger climate classification (Öztürk et al. 2017). Freeze-thaw processes occurring especially during the winter season, gravity on high slope areas, and the general lithology of the study area containing volcanic rocks with intensely fractured structure play large roles in triggering rockfall events (Fig. 2). Rockfall events are mostly experienced on high-slope areas located south of the village (Fig. 1d). The slopes of areas where rockfall events occur vary from 23–90° and the area has a convex profile.

Datasets And Processing

Accurate analysis is required due to the high hazard and risk status of rockfalls. From this aspect, modelling studies have great importance (Mary Vick et al. 2019). For rockfall modelling studies, geomorphometric approaches and modelling based on high-resolution DSM data provide more accurate and sensitive results (Loye et al. 2009; Zhang et al. 2019; Pérez-Rey et al. 2019; Francioni et al. 2020; Rodriguez et al. 2020; Akın et al. 2021). Within this scope, UAVs offer significant advantages in producing DSM and orthophoto data for large areas in a short duration and gain great importance for monitoring the distribution of natural disasters, especially, in spatial and temporal terms (Feng and Röshoff 2004;

Abellán et al. 2006; Armesto et al. 2009; Alejano et al. 2013; Giordan et al. 2015). High-resolution DSM and orthophoto data are very effective for accurate and sensitive creation of trajectory analyses and detection of source zones in rockfall studies. For this reason, rockfall studies in recent years have moved beyond traditional methods (Colomina and Molina 2014; Boccardo et al. 2015; Gomez and Purdie 2016; Manconi et al. 2019) and begun to use high-resolution digital elevation model (DEM) and orthophoto data obtained with UAVs (Matasci et al. 2015; Török et al. 2017; Byrne 2018; Manconi et al. 2019).

3.1. UAV Survey and Photogrammetric processing

A DJI Phantom 4 Advanced UAV was used to produce high-resolution orthophoto and digital surface models for rockfall modelling. The general flowchart followed when producing this data is given in Fig. 3.

Preparations for flight height, scanning width and stereo image matching proportions were completed with Pix4dcapture software for the study area. With the aim of producing DSM and orthophoto data with good quality and sensitivity, 40 ground control points (GCP) were placed with D-GPS before the flight. Five parallel flights were made at 100 meters height, and 621 stereo aerial photographs were obtained with 70% overlap ratio (Fig. 4a-b). Processing of these images used the Pix4d program trial version. In the study using 40 GCP, DSM and orthophoto images with low 1.4 cm RMSE error and 3.03 cm resolution were obtained (Fig. 4c-d).

3.2. Rockfall simulations

A range of rockfall models were developed in order to assess rockfalls in terms of dynamics, trajectories, kinetic energies, velocity and bounce heights and many other aspects, (Azzoni et al. 1995; Dorren 2003; Volkwein et al. 2011; Frattini et al. 2012; Žabota et al. 2021; Liu et al. 2021). Digital modelling like RAMMS, CONEFALL, STONE, Georock, Rockyfor3D, FlowR and Rotomap produce two-dimensional (2D) and 3D rockfall models based on geographical information systems (GIS) (Guzzetti et al. 2002; Jaboyedoff and Labiouse 2011; Topal et al. 2012; Bartelt et al. 2016a). 3D modelling studies are performed by identifying source zones, fall tracks and runout zones for rockfalls (Dorren 2003). It is important to assess modelling results linked to detection of blocks with rockfall potential within the scope of hazards and risks of properties like trajectory, velocity, kinetic energy and bounce height (Dorren 2003; Volkwein et al. 2011; Bartelt et al. 2016b; Zygouri and Koukouvelas 2017). Results obtained from this modelling provide advantages in producing hazard maps for rockfall susceptibility, protection, vulnerability, frequency, failure, distribution, etc. (Vo 2015; Bonneau et al. 2018; Sarro et al. 2018; Singh et al. 2018; Sazid 2019). For this reason, implementing the necessary protective systems (fences, ditches and forests) as a result of modelling by identifying these blocks and performing the necessary measurements may prevent these hazards and risks (Piacentini and Soldati 2008).

In this study, blocks identified in field studies with high hazard and risk had 3D analyses completed with the RAMMS program. After obtaining high-resolution orthophoto and DSM data, field studies were completed to identify blocks with fall hazard and perform dimensional measurements. During these field studies, 17 blocks with fall hazard identified (Fig. 5–6) and the height, width and length measurements

were performed for these rocks (Table 1). After determining the geometric and volumetric properties of these rocks, with very different shapes and volumes, 3D rockfall analysis for the rocks were completed with the RAMMS-Rockfall program which is a GIS-based rockfall simulation program (Leine et al. 2014; Bartelt et al. 2016a). This program provides a great advantage for accurate and high-quality modelling of rocks with different shapes and volumes measured in field studies (Mary Vick et al. 2019).

In the rock modelling process, a range of data inputs are required in addition to modelling obtained linked to DEM data. These inputs include features like plant cover (open, dense, etc.), terrain types (hard, extra hard, medium, soft, medium soft, etc.), and block types (flat, equitant, round, etc.) for blocks or source zone areas to be modelled by the RAMMS program (Vo 2015). For rock modelling in the RAMMS program, DEM data with resolution from 1–10 m is sufficient. For this reason, DSM data with cm-resolution was rescaled to 1 meter resolution to obtain the format for use in modelling. Based on the volcanic rocks in the general geology of the field, the terrain type was selected as hard terrain, covered with very sparse plant cover (Fig. 4c).

Table 1
Geometric properties of the simulated rocks

No	X (length) m	Y (width) m	Z (height) m	Volume m^3	Mass kg	Rock shape
R1	3.2	2.5	1.5	7.96	21485.4	Equant
R2	2.0	1.8	1.0	1.545	4172.5	Equant
R3	1.5	1.6	1.2	0.719	1941.7	Real long
R4	1.42	1.23	1.0	0.95	2565.2	Real Equant
R5	1.2	1.4	0.8	0.925	2497.8	Real Flat
R6	1.5	1.25	1.0	1.124	3035.6	Equant
R7	1.5	1.25	1.0	1.124	3035.6	Equant
R8	1.22	1.17	1.0	0.687	1856	Real Flat
R9	0.96	1.16	0.98	0.464	1253.5	Real Long
R10	1.42	1.23	1.0	0.950	2565.2	Real Equant
R11	1.42	1.23	1.0	0.950	2565.2	Real Equant
R12	1.15	1.49	1.0	0.698	1.885	Real Long
R13	3.24	1.62	2.23	0.524	1414.1	Real Long
R14	1.56	2.01	1.35	0.719	1941.7	Real Long
R15	1.42	1.23	1.0	0.950	2565.2	Real Equant
R16	1.61	1.34	1.07	1.124	3035.6	Equant
R17	2.18	2.34	1.87	1.242	3352.4	Real Equant

3.3. Rockfall Hazard Index

Hazard mapping for rockfalls used the “Rockfall Hazard Index” (RHI) method (Crosta and Agliardi 2003). In this method, the kinetic energy, jump height and block count features are noted and the RAMMS program is used to create these basic parameters. Basic parameters are reclassified within the scope of hazards. During the reclassification, the classification values of Crosta and Agliardi (2003) were used. Necessary classifications for kinetic energy, bounce height and block count values are presented in Table 1. For calculation of block count value, the c/(5*n) formula was used and then reclassification was performed. In the formula, c: rockfall count, and n: number of blocks launched from each cell value. The values obtained within this scope were separately calculated for reach rockfall model with the results of classification of the 3 parameters combined to identify high-moderate-low hazard areas.

Table 2
Classification of parameters according to the rockfall hazard index method (Crosta and Agliardi, 2003).

Class	Block count (local scale)	Kinetic energy (kJ)	Jump height (m)
1	< 0.01	≤ 700	≤ 4
2	0.01–0.1	700–2500	4–10
3	> 0.1	≥ 2500	≥ 10

Results

The heights of these blocks determined as a result of field studies varied from 0.8-2/23 m, with lengths from 0.96–3.2 m and widths of 1.16–2.5 m (Fig. 6). According to models obtained by defining these measured dimensions in the RAMMS program, the volumes of the blocks varied from 7.96 m^3- 0.46 m^3, while masses varied from 214,485 kg-1253 kg. According to the measured values, the block shapes were identified as equant, real long, real equant and real flat. According to these features defined in the RAMMS program, 100 repeats for each of the 17 blocks were modelled for a total of 1700 blocks. As a result of this modelling, the kinetic energy (kJ), velocity (m/s), jump height (m) and rockfall hazard index features were determined for each block.

Rocks display variations in the distance covered after falls linked to the shape and volume of the block, in addition to being shaped by the features of the slope. As understood from the values obtained accordingly, on vertical and high-slope areas where slope values are high but discontinuous, blocks stop before being transported a very advanced distance. This situation is clearly observed for blocks R2, R3, R5 and R6 and the slope values for these rocks are generally above 46°, equivalent to vertical slopes and high cliffs. For rocks in areas where the slope values are continuous, blocks appear to be transported over very long distances. As seen for blocks R1, R4, R6, R7, R8, R9, R10, R11, R12, R14, R15, R16, and R17, variable rounding features are present according to the geometry of the blocks. Apart from this, R12 block has a continuous slope profile; however, the block could not progress a long distance due to the different shape (real long).

There is a parallel between the kinetic energy released and the volume and geometry of the block and the continuity of slope values. Fall properties of blocks R2, R3, R4, R5 and R6 had mean 479 kJ kinetic energy, rising to a maximum of 1183 kJ. Other rocks with more rounded features (R1-R6-R7-R8-R9-R10-R11-R12) had mean 726 kJ kinetic energy reaching a maximum of 3476 kJ (Fig. 7).

While the geometric properties of the rocks play an important role in their progression, the geomorphology of the field in which the rockfall event occurs is also effective. Generally, the trajectories of blocks are shown on red relief images in order to better understand the slope features and general topographic characteristics of the study area in general. Accordingly, the modelling for R2, R3, R4, R5 and R6 appear to

show they are channelled into valleys and do not reach the settlement area and model results generally end in the middle of the valley. Apart from these, it appears that modelling of blocks with lower slope rates and without narrow or deep values in geomorphological terms affect settlement areas more and leave them at risk (Fig. 7).

Just as the geometric shapes of rocks and slope features of the area affect the kinetic energy, they directly affect the rock velocity and the bounce height. Generally, high velocities and jump heights are equivalent to areas where kinetic energy reaches maximum levels. As a result of modelling for 17 different rock blocks, maximum velocities were 8.1–23.1 m/s. Maximum bounce heights varied from 1.9 m to 14.5 m (Table 1). The block with lowest value appeared to be block number R4 with real flat geometry (Table 2).

4.1. Rockfall Hazard Assessment

The trajectories and values emerging as a result of block modelling involve great hazards for settlement units. Rockfalls from vertical and close-to-vertical steep slopes generally stop on roads and there is no contact with settlement units. However, apart from blocks number R2, R3 and R5, it appears that damage to residential units is unavoidable in modelling of the rockfall of 14 different blocks. Apart from these, blocks with rounded features cause some completely different outcomes to emerge. These rocks have very high-risk status due to being transported over long distances. It appears they may cause great damage and even loss of life due to high energy, velocity and bounce features. The hazard status emerging as a result of modelling of blocks identified based on field studies in the study area are included in Table 2.

Table 2
Results for blocks with fall hazard (H: House, T: Tree, R: Road)

No	Max. kinetic energy (kJ)	Max. velocity (m/s)	Max. jump height (m)	Max. distance travelled (m)	Element at risk
R1	3476.8	16.73	5.25	127.5	H,T,R
R2	1183.5	14.53	4.25	85	T,R
R3	160.6	10.15	2.27	97	H,T,R
R4	383.1	16.46	5.75	112	H,T,R
R5	90.6	8.17	1.99	75	
R6	581	17.9	9.02	87	H,T
R7	131	17.19	8.71	55	Abandoned H
R8	397.5	19.93	7.83	120	H,T,R
R9	185.2	16.51	6.84	85	H,T,R
R10	285.4	13.71	6.05	84	H,T,R
R11	701	23.1	14.57	87	H,T,R
R12	166	12.06	4.1	56	H,T
R13	630	8.74	4.55	34	H
R14	441	13	6.23	45	H
R15	312	14.63	6.42	67	H,T,R
R16	257.4	10.61	3.04	53	H,T
R17	1737.6	16.05	10.1	70	H,T,R

According to the hazard map, modelling of rocks R6, R12, R13, R14, R15, R16 and R17 show the majority of high and moderate risk areas are settlement areas. Modelling of blocks R1, R4, R7, R8, R9 and R10 show the majority involve low hazard, while a small portion involve moderate degree of hazard (Fig. 8).

Conclusion

In this study, 17 rock blocks determined to have high hazard and risk in field studies were modelled for rockfall risk with high resolution UAV-DEM data for Hacıabdullah village, where rockfall events are continuously experienced. According to the model results, the maximum kinetic energy was identified as 3476 kJ, maximum velocity was 23.1 m/s and maximum jump height was 14.57 m. These values show variation according to the general slope values for the study area, the slope profile and geomorphology of the rockfall area, and the geometry and volume of the blocks. Blocks may travel very long distances in

regions with slope values below 46°, while blocks stop on slope breaks without travelling long distances when slope values are from 46–90°. Models for blocks channelled into valleys ended within the valley. However, models for rocks found on ridges show large areas are threatened. According to the hazard map, blocks R6, R12, R13, R14, T15, R16 and R17 involve high and moderate levels of risk for settlement units. Taking the necessary precautions for the determined risk areas has vital importance due to the frequent experience of rockfalls in the area. The model outcomes should be considered when taking the necessary precautions. In conclusion, in Hacıabdullah village where rockfall events are actively experienced, risk for settlement areas and the spatial distribution of this risk were accurately revealed by field study results and rockfall models completed with a high-resolution digital elevation model produced with the aid of a UAV. These results have great importance in terms of taking the necessary precautions.

Declarations

Ethical Statements

Conflicts of Interest: The author declares no conflict of interest.

Funding: This research received no external funding.

References

1. Abebe B, Dramis F, Fubelli G et al (2010) Landslides in the Ethiopian highlands and the Rift margins. J African Earth Sci 56:131–138. https://doi.org/10.1016/j.jafrearsci.2009.06.006
2. Abellán A, Vilaplana JM, Martínez J (2006) Application of a long-range Terrestrial Laser Scanner to a detailed rockfall study at Vall de Núria (Eastern Pyrenees, Spain). Int J Rock Mech Min Sci Geomech 88:136–148. https://doi.org/10.1016/j.enggeo.2006.09.012
3. Akın M, Dinçer İ, Ok A et al (2021) Assessment of the effectiveness of a rockfall ditch through 3-D probabilistic rockfall simulations and automated image processing. Eng Geol 283:106001. https://doi.org/10.1016/j.enggeo.2021.106001
4. Akın M, Dinçer İ, Orhan A et al (2019) Evaluation of the Performance of a Rockfall Ditch by 3-Dimensional Rockfall Analyses: Akköy (Ürgüp) Case. Jeol Muhendisligi Derg 43:211–232. https://doi.org/10.24232/jmd.655005
5. Alejano LR, García-Cortés S, García-Bastante F, Martínez-Alegría R (2013) Study of a rockfall in a limy conglomerate canyon (Covarrubias, Burgos, N. Spain). Environ Earth Sci 70:2703–2717. https://doi.org/10.1007/s12665-013-2327-x
6. Armesto J, Ordóñez C, Alejano L, Arias P (2009) Terrestrial laser scanning used to determine the geometry of a granite boulder for stability analysis purposes. Geomorphology 106:271–277. https://doi.org/10.1016/j.geomorph.2008.11.005
7. Ashfield JR (2001) The computer simulation and prediction of rock fall by. Durham theses, Durham University. Available at Durham E-Theses Online: http://etheses.dur.ac.uk/4383/ Use

8. Aydın A, Eker R (2017) Kaya yuvarlanmalarından etkilenen orman alanlarının belirlenmesi: İnebolu örneği. İstanbul Üniversitesi. Orman Fakültesi Derg 67:136–149. https://doi.org/10.17099/jffiu.281710
9. Azzoni A, La Barbera G, Zaninetti A (1995) Analysis and prediction of rockfalls using a mathematical model. Int J Rock Mech Min Sci 32:709–724. https://doi.org/10.1016/0148-9062(95)00018-C
10. Baillifard F, Jaboyedoff M, Sartori M (2010) Rockfall hazard mapping along a mountainous road in Switzerland using a GIS-based parameter rating approach. Nat Hazards Earth Syst Sci 3:435–442. https://doi.org/10.5194/nhess-3-435-2003
11. Bartelt P, Bieler C, Bühler Y et al (2016a) RAMMS::ROCKFALL User Manual v1.6. 102
12. Bartelt P, Gerber W, Christen M, Bühler Y (2016b) Modeling rockfall trajectories with non-smooth contact/impact mechanics. In: 13th Congress Interpraevent 2016. pp 203–211
13. Berger F, Rey F (2004) Mountain protection forests against natural hazards and risks: New french developments by integrating forests in risk zoning. Nat Hazards 33:395–404. https://doi.org/10.1023/B:NHAZ.0000048468.67886.e5
14. Boccardo P, Chiabrando F, Dutto F et al (2015) UAV Deployment Exercise for Mapping Purposes: Evaluation of Emergency Response Applications. Sensors 15:15717–15737. https://doi.org/10.3390/s150715717
15. Bonneau DA, Hutchinson DJ, Difrancesco P et al (2018) 3-Dimensional Rockfall Shape Back-Analysis: Methods and Implications. 1–35. https://doi.org/https://doi.org/10.5194/nhess-2018-366
16. Bull WB, King J, Kong F et al (1994) Lichen dating of coseismic landslide hazards in alpine mountains. Geomorphology 10:253–264
17. Byrne K (2018) Digital Morphometry Applied to Geo-Hazard Risk Assessment: A Case Study from Germany. Technische Universitat Dresden. Faculty of Environmental Sciences, Institute for Cartography, Master of Science
18. Colomina I, Molina P (2014) Unmanned aerial systems for photogrammetry and remote sensing: A review. ISPRS J Photogramm Remote Sens 92:79–97. https://doi.org/10.1016/j.isprsjprs.2014.02.013
19. Crosta GB, Agliardi F (2003) A methodology for physically based rockfall hazard assessment. Nat Hazards Earth Syst Sci 3:407–422. https://doi.org/10.5194/nhess-3-407-2003
20. Cybulski PG (2014) Rock Fall Mitigation for an Open. Pit Mine Experiencing Substantial
21. Dinçer İ, Orhan A, Frattini P, Crosta GB (2016) Rockfall at the heritage site of the Tatlarin Underground City (Cappadocia, Turkey). Nat Hazards 82:1075–1098. https://doi.org/10.1007/s11069-016-2234-z
22. Dorren LKA (2003) A review of rockfall mechanics and modelling approaches. Prog Phys Geogr 27:69–87. https://doi.org/10.1191/0309133303pp359ra
23. Dorren LKA, Maier B, Putters US, Seijmonsbergen AC (2004) Combining field and modelling techniques to assess rockfall dynamics on a protection forest hillslope in the European Alps. Geomorphology 57:151–167. https://doi.org/10.1016/S0169-555X(03)00100-4

24. Dorren LKA, Seijmonsbergen AC (2003) Comparison of three GIS-based models for predicting rockfall runout zones at a regional scale. Geomorphology 56:49–64. https://doi.org/10.1016/S0169-555X(03)00045-X
25. Evans SG, Hungr O (1993) The assessment of rockfall hazard at the base of talus slopes. Can Geotech J 30:620–636. https://doi.org/10.1139/t93-054
26. Feng QH, Röshoff K (2004) In-situ mapping and documentation of rock faces using a full-coverage 3d laser scanning technique. Int J Rock Mech Min Sci 41:1–6. https://doi.org/10.1016/j.ijrmms.2004.03.032
27. Fityus SG, Giacomini A, Buzzi O (2013) The significance of geology for the morphology of potentially unstable rocks. Eng Geol 162:43–52. https://doi.org/10.1016/j.enggeo.2013.05.007
28. Francioni M, Antonaci F, Sciarra N et al (2020) Application of Unmanned Aerial Vehicle Data and Discrete Fracture Network Models for Improved Rockfall Simulations. Remote Sens 12:2053. https://doi.org/10.3390/rs12122053
29. Frattini P, Crosta GB, Agliardi F (2012) Rockfall characterization and modeling. In: Clague JJ, Stead D (eds) Landslides. Cambridge University Press, Cambridge, pp 267–281
30. Geniş M, Sakız U, Çolak Aydıner B (2017) A stability assessment of the rockfall problem around the Gökgöl Tunnel (Zonguldak, Turkey). Bull Eng Geol Environ 76:1237–1248. https://doi.org/10.1007/s10064-016-0907-1
31. Giordan D, Manconi A, Facello A et al (2015) Brief Communication: The use of an unmanned aerial vehicle in a rockfall emergency scenario. Nat Hazards Earth Syst Sci 15:163–169. https://doi.org/10.5194/nhess-15-163-2015
32. Gomez C, Purdie H (2016) UAV- based Photogrammetry and Geocomputing for Hazards and Disaster Risk Monitoring – A Review. Geoenvironmental Disasters 3:. https://doi.org/10.1186/s40677-016-0060-y
33. Gül M, Özbek A, Karacan E (2016) Rock fall hazard assessment in Asar Hill, ancient Mabolla City, Mugla—SW Turkey. Environ Earth Sci 75:1310. https://doi.org/10.1007/s12665-016-6113-4
34. Guzzetti F, Crosta G, Detti R, Agliardi F (2002) STONE: A computer program for the three-dimensional simulation of rock-falls. Comput Geosci 28:1079–1093. https://doi.org/10.1016/S0098-3004(02)00025-0
35. Jaboyedoff M, Labiouse V (2011) Technical note: Preliminary estimation of rockfall runout zones. Nat Hazards Earth Syst Sci 11:819–828. https://doi.org/10.5194/nhess-11-819-2011
36. Kayabaşı A (2018) The assesment of rockfall analysis near a railroad: a case study at the Kızılinler village of Eskişehir, Turkey. Arab J Geosci 11:800. https://doi.org/10.1007/s12517-018-4175-1
37. Leine RI, Schweizer A, Christen M et al (2014) Simulation of rockfall trajectories with consideration of rock shape
38. Liu G, Li J, Wang Z (2021) Experimental Verifications and Applications of 3D-DDA in Movement Characteristics and Disaster Processes of Rockfalls. Rock Mech Rock Eng. https://doi.org/10.1007/s00603-021-02394-2

39. Loye A, Jaboyedoff M, Pedrazzini A (2009) Identification of potential rockfall source areas at a regional scale using a DEM-based geomorphometric analysis. Nat Hazards Earth Syst Sci 9:1643–1653. https://doi.org/10.5194/nhess-9-1643-2009
40. Lu G, Caviezel A, Christen M et al (2019) Modelling rockfall impact with scarring in compactable soils. Landslides 16:2353–2367. https://doi.org/10.1007/s10346-019-01238-z
41. Manconi A, Ziegler M, Blöchliger T, Wolter A (2019) Technical note: optimization of unmanned aerial vehicles flight planning in steep terrains. Int J Remote Sens 40:2483–2492. https://doi.org/10.1080/01431161.2019.1573334
42. Mary Vick L, Zimmer V, White C et al (2019) Significance of substrate soil moisture content for rockfall hazard assessment. Nat Hazards Earth Syst Sci 19:1105–1117. https://doi.org/10.5194/nhess-19-1105-2019
43. Matasci B, Jaboyedoff M, Loye A et al (2015) Impacts of fracturing patterns on the rockfall susceptibility and erosion rate of stratified limestone. Geomorphology 241:83–97. https://doi.org/10.1016/j.geomorph.2015.03.037
44. Matsuoka N (1999) Rockfall activity from an alpine cliff during thawing periods. Geomorphology 28:309–328
45. Mccarroll D, Shakesby RA, Matthews JA et al (1998) Spatial and Temporal Patterns of Late Holocene Rockfall Activity on a Norwegian Talus Slope: of Late Holocene Rockfall on a Patterns. Spatial Temporal Activity Talus a Lichenometric and Norwegian Slope : Approach
46. Öztürk MZ, Çetinkaya G, Aydın S (2017) Köppen-Geiger İklim Sınıflandırmasına Göre Türkiye'nin İklim Tipleri. Coğrafya Derg 17–27 (In Turkish)
47. Pérez-Rey I, Riquelme A, González-deSantos LM et al (2019) A multi-approach rockfall hazard assessment on a weathered granite natural rock slope. Landslides 16:2005–2015. https://doi.org/10.1007/s10346-019-01208-5
48. Piacentini D, Soldati M (2008) Application of empiric models for the analysis of rock-fall runout at a regional scale in mountain areas: Examples from the dolomites and the northern apennines (Italy). Geogr Fis e Din Quat 31:215–223
49. Rodriguez J, Macciotta R, Hendry MT et al (2020) UAVs for monitoring, investigation, and mitigation design of a rock slope with multiple failure mechanisms—a case study. Landslides 17:2027–2040. https://doi.org/10.1007/s10346-020-01416-4
50. Sarro R, Carlos J, Mar R (2018) Rockfall Simulation Based on UAV Photogrammetry Data Obtained during an Emergency Declaration: Application at a Cultural Heritage Site. Remote Sens. https://doi.org/10.3390/rs10121923
51. Sazid M (2019) Analysis of rockfall hazards along NH-15: A case study of Al-Hada road. Int J Geo-Engineering 10:1–13. https://doi.org/10.1186/s40703-019-0097-3
52. Singh A, Pal S, Kanungo DP (2018) Site-Specific Vulnerability Assessment of Buildings Exposed to Rockfalls. Renew Energy its Innov Technol 1–11. https://doi.org/10.1007/978-981-13-2116-0_1

53. Singh PK, Kainthola A, Panthee S, Singh TN (2016) Rockfall analysis along transportation corridors in high hill slopes. Environ Earth Sci 75:1–11. https://doi.org/10.1007/s12665-016-5489-5
54. Taga H, Zorlu K (2016) Assessment of rockfall hazard on the steep-high slopes: Ermenek (Karaman, Turkey). Nat Hazards Earth Syst Sci Discuss 1–32. https://doi.org/10.5194/nhess-2015-337
55. Tanarro LM, Munoz J (2012) Rockfalls in the Duratón canyon, central Spain: Inventory and statistical analysis. Geomorphology 169–170:17–29. https://doi.org/10.1016/j.geomorph.2012.01.003
56. Topal T, Akın MK, Akın M (2012) Rockfall hazard analysis for an historical Castle in Kastamonu (Turkey). Nat Hazards 62:255–274. https://doi.org/10.1007/s11069-011-9995-1
57. Török Á, Barsi Á, Bögöly G et al (2017) Slope stability and rock fall hazard assessment of volcanic tuffs using RPAS and TLS with 2D FEM slope modelling. Nat Hazards Earth Syst Sci Discuss 1–30. https://doi.org/10.5194/nhess-2017-56
58. Utlu M, Öztürk MZ, Şimşek M (2020a) Rockfall analysis based on UAV technology in Kazıklıali Gorge, Aladağlar (Taurus Mountains, Turkey). Int J Environ Geoinformatics 7:239–251. https://doi.org/10.30897/ijegeo
59. Utlu M, Öztürk MZ, Şimşek M (2020b) Emli Vadisi'ndeki (Aladağlar) Talus Depolarının Kantitatif Analizlere Göre İncelenmesi. In: Birinci S, Kıvanç Kaymaz Ç, Kızılkan Y (eds) COĞRAFİ PERSPEKTİFLE DAĞ VE DAĞLIK ALANLAR (Sürdürülebilirlik-Yönetim-Örnek Alan İncelemeleri), I. Kriter Yayınevi, İstanbul-Turkey, pp 51–72
60. Utlu M, Öztürk MZ, Şimşek M (2021) Yüksek Çözünürlüklü Sayısal Yüzey Modellerine Uygulanan Üç Boyutlu Analizler ile Kaya Düşmelerine Ait Sayısal Risk Değerlendirmesi: Ünlüyaka Köyü (Niğde, Türkiye). In: Döker MF, Akköprü E (eds) COĞRAFYA ARAŞTIRMALARINDA COĞRAFİ BİLGİ SİSTEMLERİ UYGULAMALARI II, I. PEGEM AKADEMi, Ankara-Turkey, pp 51–69
61. Varnes DJ (1978) Slope Movement Types and Processes. Transp Res Board Spec Rep 11–33
62. Vidrih R, Ribicic M, Suhadolc P (2001) Seismogeological effects on rocks during the 12 April 1998 ˇ a Territory earthquake (NW Slovenia) upper Soc AR. Tectonophysics 330:153–175
63. Vijayakumar S, Yacoub T, Curran H J (2011) On the effect of rock size and shape in rockfall analyses. In: On the effect of rock size and shape inrockfall analyses. San Francisco CA, USA
64. Vo DT (2015) RAMMS:: Rockfall versus Rockyfor3D in rockfall trajectory simulations at the Community of Vik, Norway Dam Thanh Vo RAMMS :: Rockfall versus Rockyfor3D in rockfall trajectory simulations at the Community of Vik, Norway. University of Oslo, Faculty of Mathematics and Natural Sciences
65. Volkwein A, Schellenberg K, Labiouse V et al (2011) Rockfall characterisation and structural protection - A review. Nat Hazards Earth Syst Sci 11:2617–2651. https://doi.org/10.5194/nhess-11-2617-2011
66. Yılmaz I, Yıldırım M, Keskin I (2008) A method for mapping the spatial distribution of RockFall computer program analyses results using ArcGIS software. Bull Eng Geol Environ 67:547–554. https://doi.org/10.1007/s10064-008-0174-x

67. Youssef AM, Pradhan B, Al-Kathery M et al (2015) Assessment of rockfall hazard at Al-Noor Mountain, Makkah city (Saudi Arabia) using spatio-temporal remote sensing data and field investigation. J African Earth Sci 101:309–321. https://doi.org/10.1016/j.jafrearsci.2014.09.021
68. Žabota B, Mikoš M, Kobal M (2021) Rockfall Modelling in Forested Areas: The Role of Digital Terrain Model Grid Cell Size. Appl Sci 11:1461. https://doi.org/10.3390/app11041461
69. Zhang Y, Yue P, Zhang G et al (2019) Augmented Reality Mapping of Rock Mass Discontinuities and Rockfall Susceptibility Based on Unmanned Aerial Vehicle Photogrammetry. Remote Sens 11:1311. https://doi.org/10.3390/rs11111311
70. Zygouri V, Koukouvelas I (2017) Techniques of rockfall inventory in earthquake prone rock slopes. Bull Geol Soc Greece 50:1756. https://doi.org/10.12681/bgsg.11899

Figures

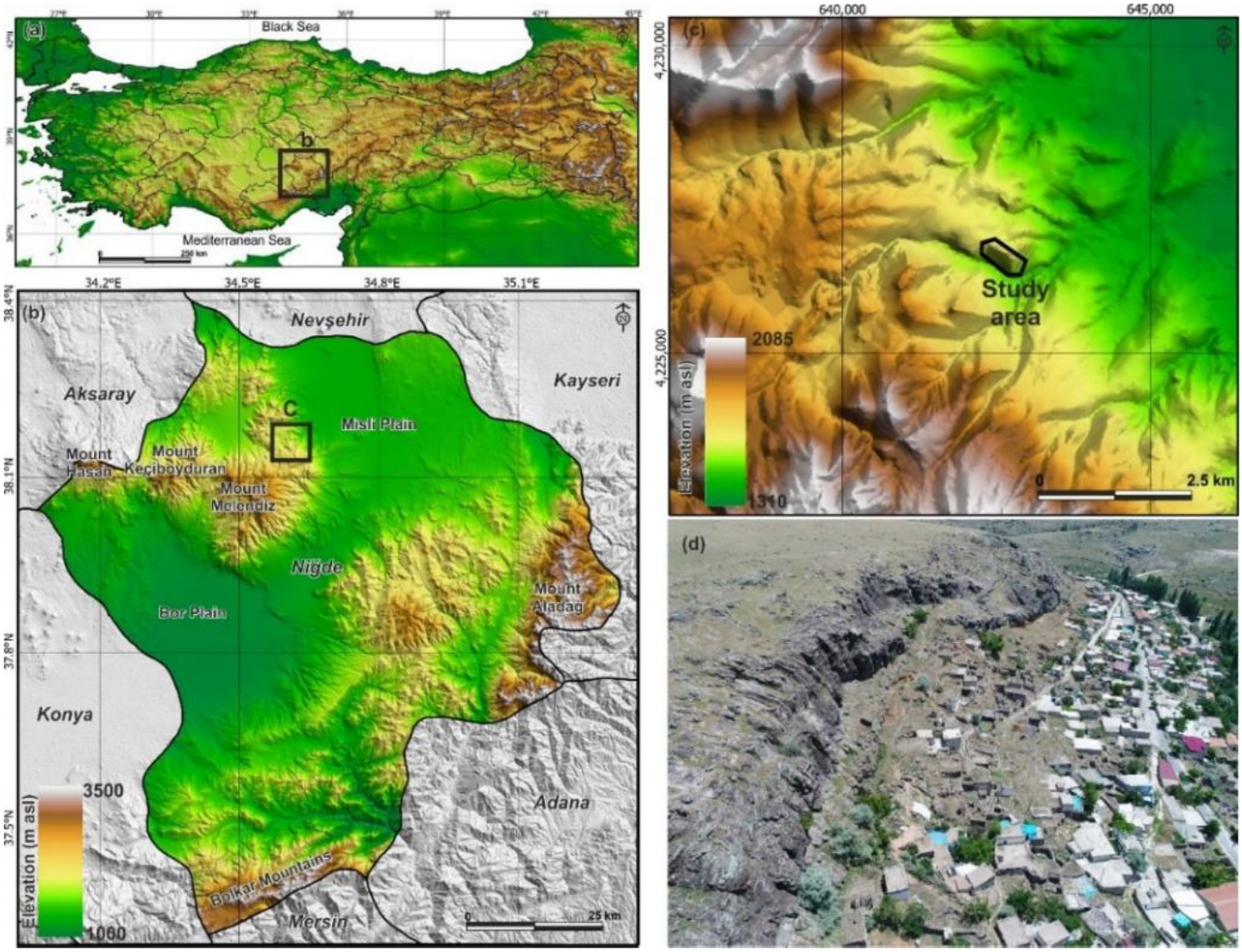

Figure 1

a-c) Location of the study area and (d) oblique aerial photograph of the study area.

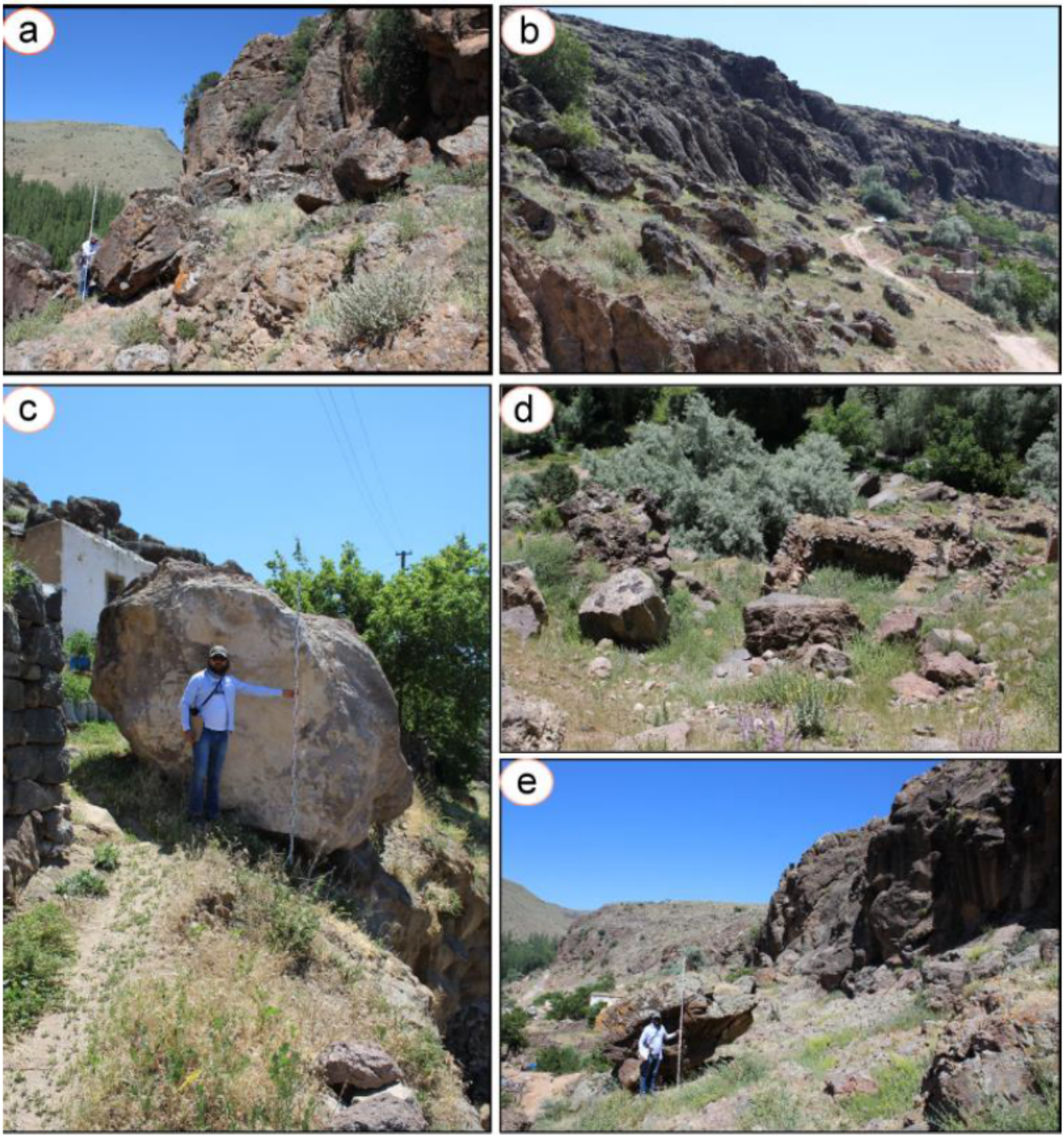

Figure 2

Fallen blocks in different sections of the village

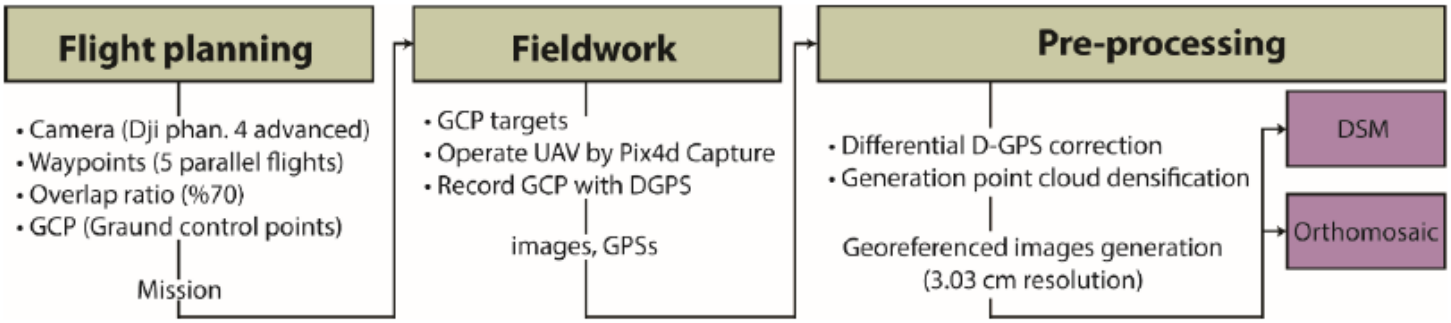

Figure 3

General flowcharts for DSM and orthomosaic generation steps

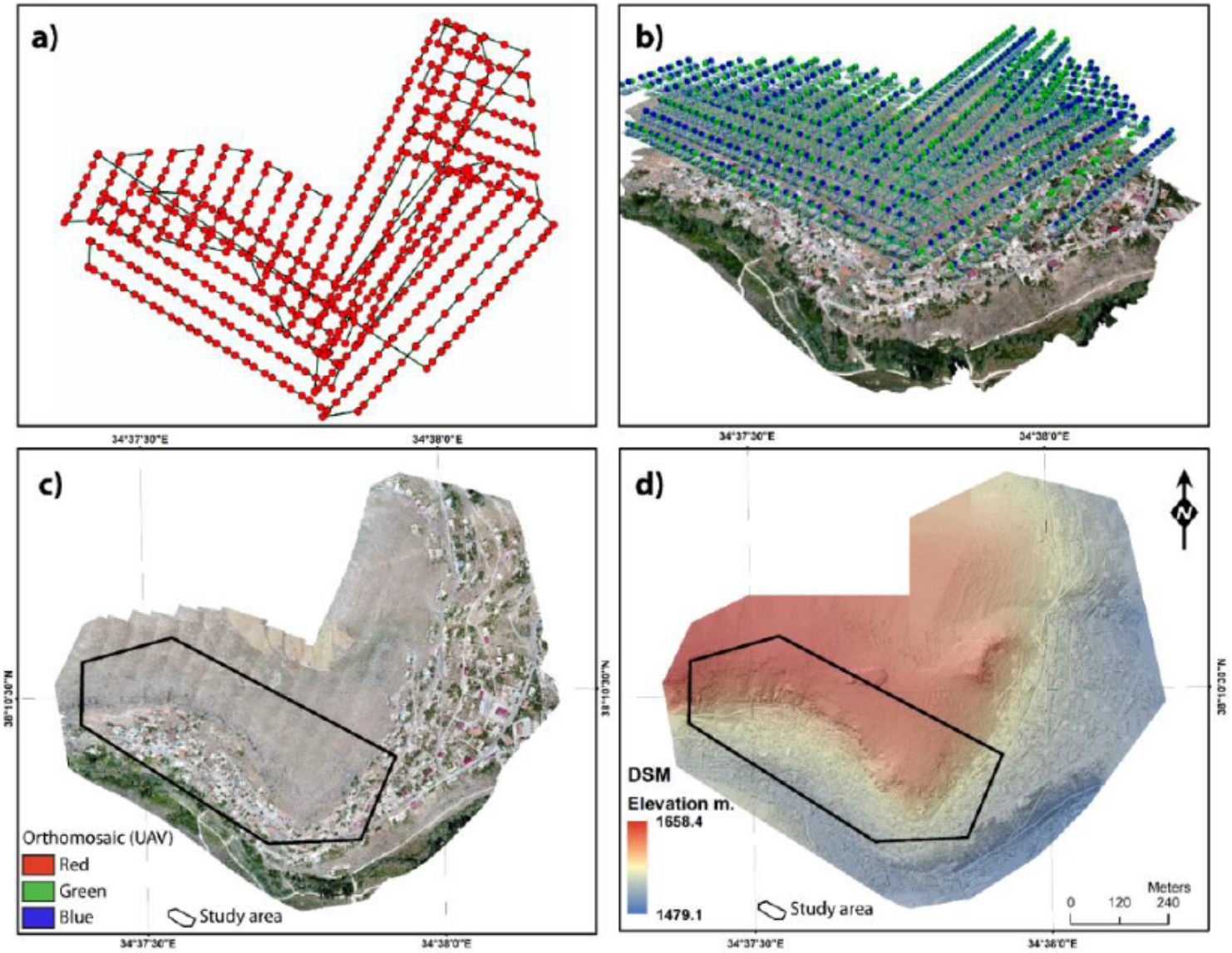

Figure 4

a) Obtaining stereo images of the planned flight path and location b) view represents the area of each image taken along the flight path and point cloud c) The orthomosaic images obtained from photogrammetric processing d) Digital surface model of the study area (3 cm resolution).

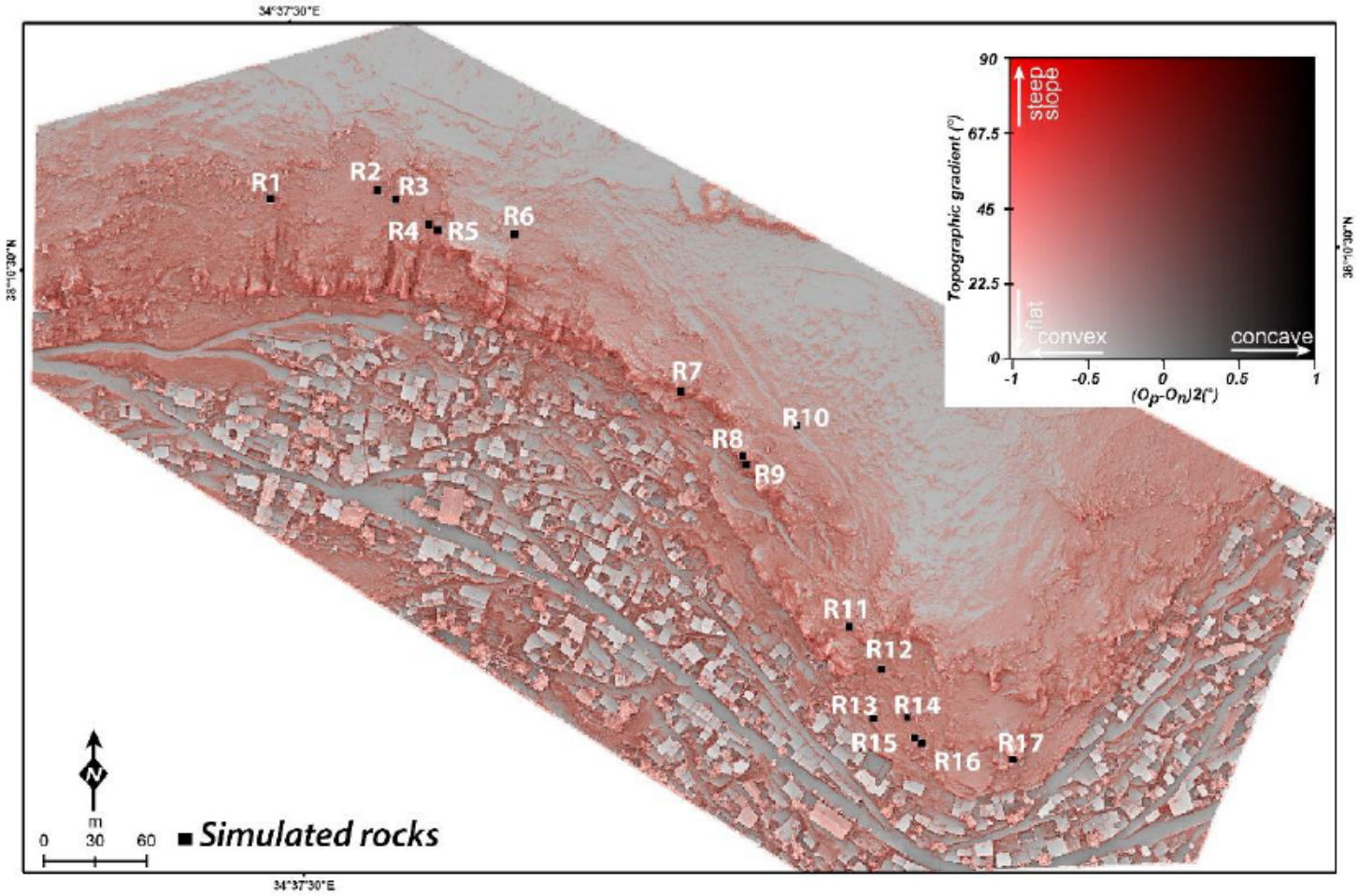

Figure 5

Red Relief Image Map (RRIM) of the study area and distribution of rocks identified in field studies

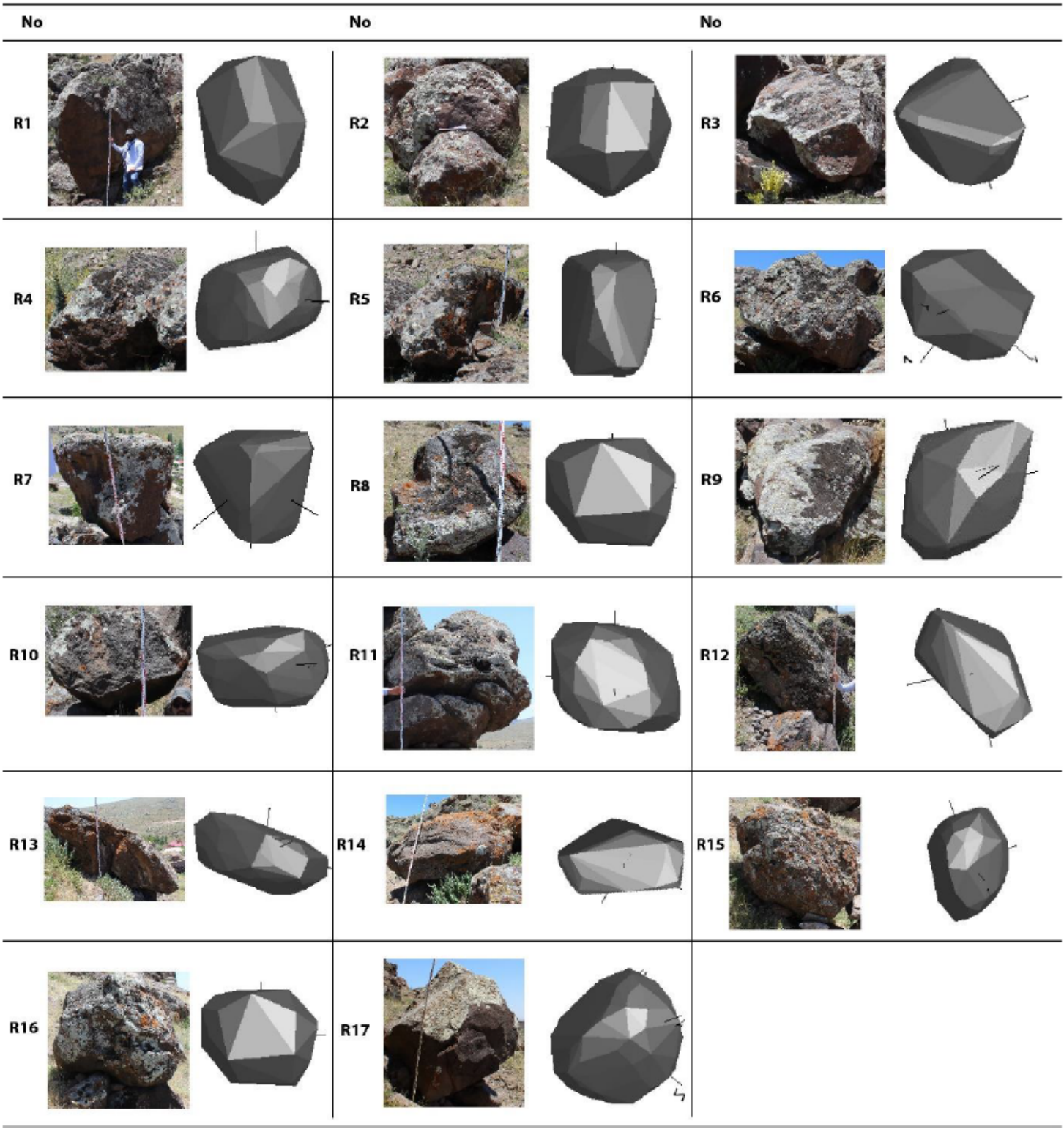

Figure 6

Photographs of rocks identified in field studies and model forms of these rocks in the RAMMS program according to dimensions measured in the field.

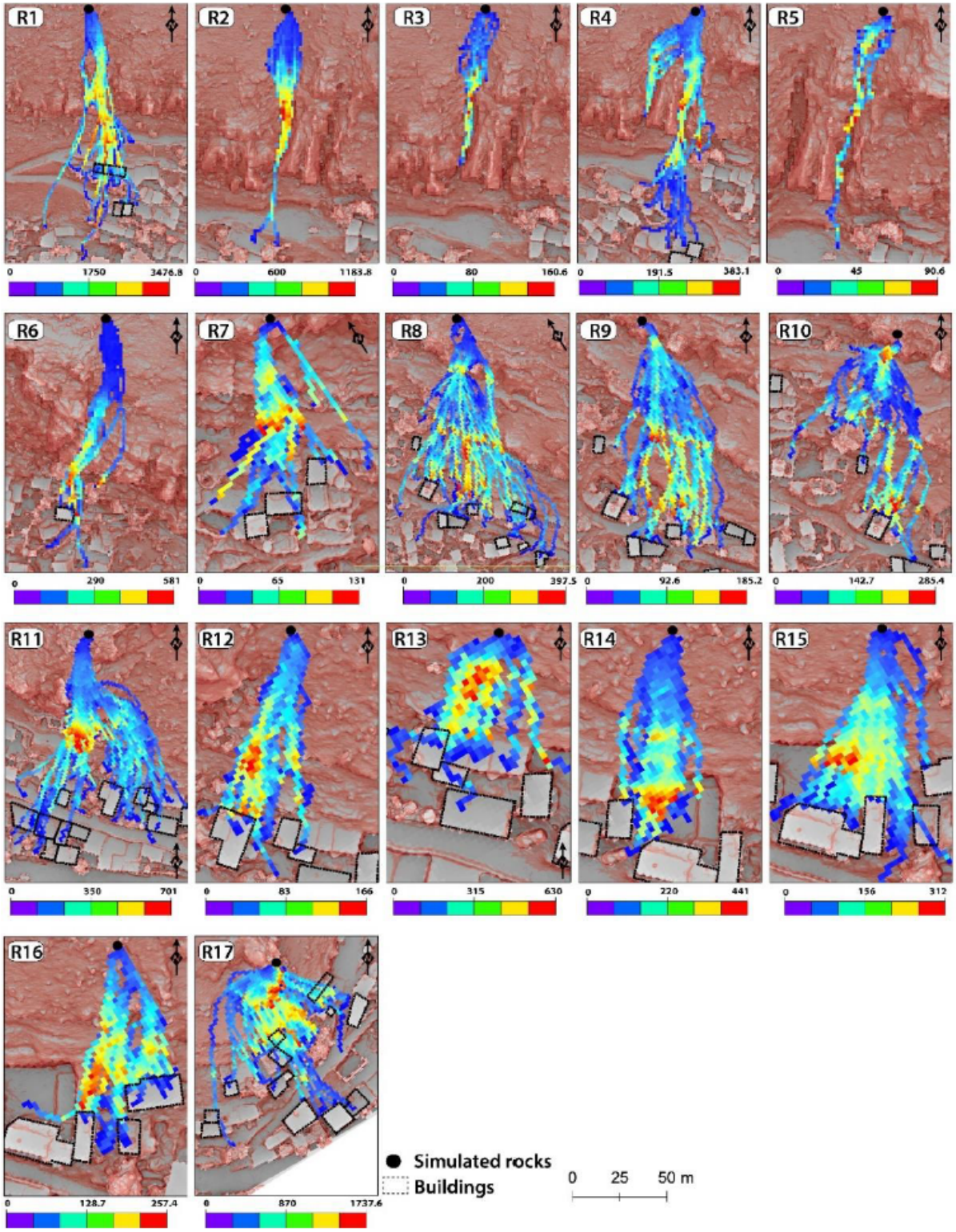

Figure 7

Trajectory and kinetic energy results for the 17 blocks

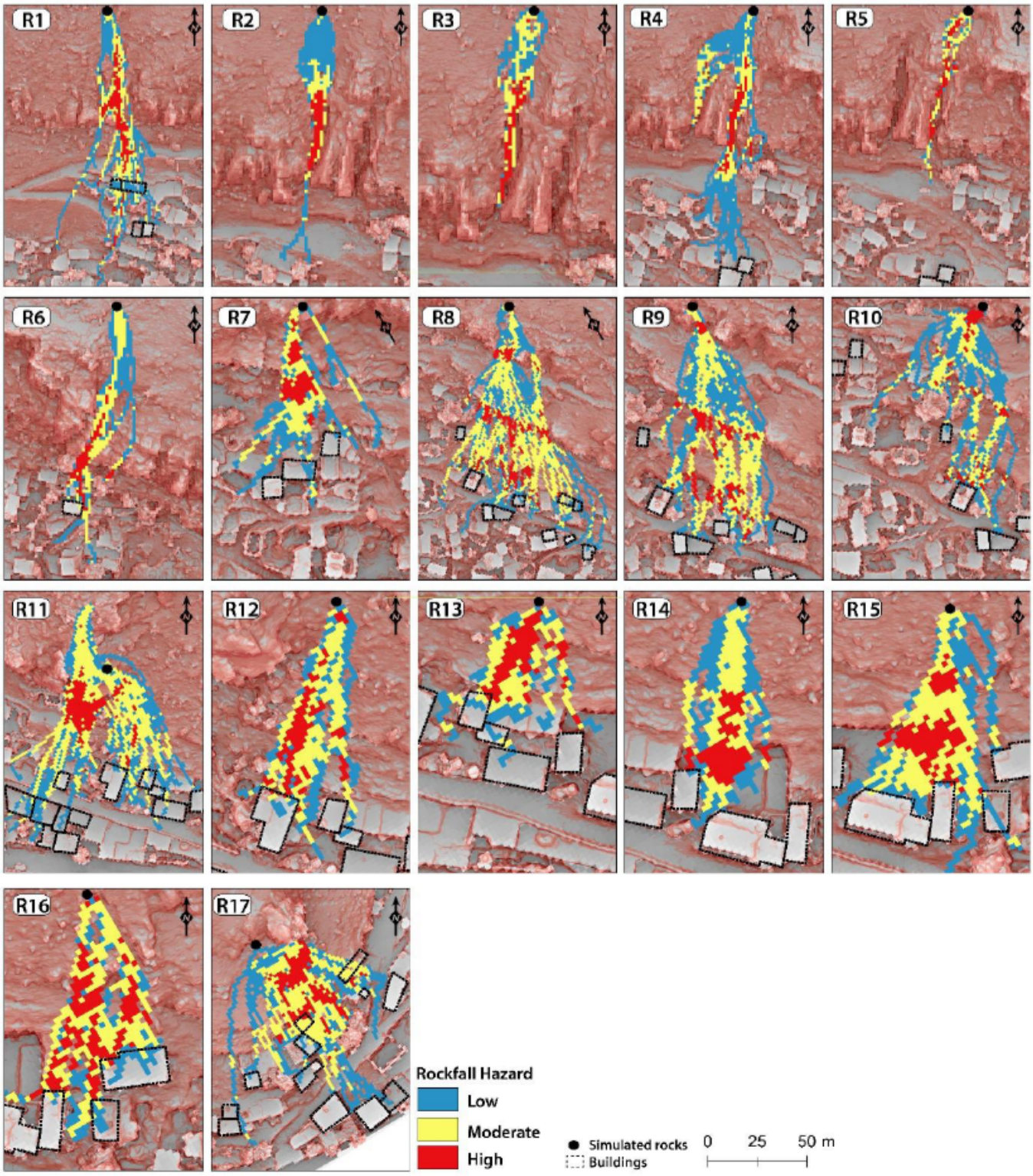

Figure 8

Rockfall Hazard Index for each block.